

X-ray monochromator with an energy resolution of 8×10^{-9} at 14.41 keV

Makina Yabashi, Kenji Tamasaku, Seishi Kikuta, and Tetsuya Ishikawa

Citation: [Review of Scientific Instruments](#) **72**, 4080 (2001); doi: 10.1063/1.1406925

View online: <https://doi.org/10.1063/1.1406925>

View Table of Contents: <http://aip.scitation.org/toc/rsi/72/11>

Published by the [American Institute of Physics](#)

Articles you may be interested in

[Development of speckle-free channel-cut crystal optics using plasma chemical vaporization machining for coherent x-ray applications](#)

[Review of Scientific Instruments](#) **87**, 063118 (2016); 10.1063/1.4954731

[Rocking curve imaging of high quality sapphire crystals in backscattering geometry](#)

[Journal of Applied Physics](#) **121**, 044901 (2017); 10.1063/1.4974106

[Ultrafast observation of lattice dynamics in laser-irradiated gold foils](#)

[Applied Physics Letters](#) **110**, 071905 (2017); 10.1063/1.4976541

[Calibration and characterization of a highly efficient spectrometer in von Hamos geometry for 7-10 keV x-rays](#)

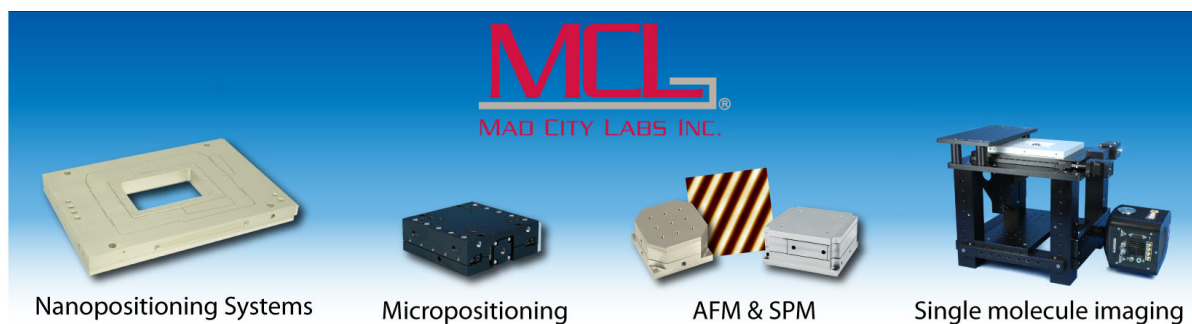
[Review of Scientific Instruments](#) **88**, 043110 (2017); 10.1063/1.4981793

[Femtosecond time-resolved X-ray absorption spectroscopy of anatase TiO₂ nanoparticles using XFEL](#)

[Structural Dynamics](#) **4**, 044033 (2017); 10.1063/1.4989862

[Construction of a precision diffractometer for nuclear Bragg scattering at the Photon Factory](#)

[Review of Scientific Instruments](#) **63**, 1015 (1992); 10.1063/1.1143188



X-ray monochromator with an energy resolution of 8×10^{-9} at 14.41 keV

Makina Yabashi^{a)}

SPring-8/JASRI, Mikazuki, Hyogo 679-5198, Japan

Kenji Tamasaku

SPring-8/RIKEN, Mikazuki, Hyogo 679-5148, Japan

Seishi Kikuta

SPring-8/JASRI, Mikazuki, Hyogo 679-5198, Japan

Tetsuya Ishikawa

SPring-8/JASRI, Mikazuki, Hyogo 679-5198, Japan
and *SPring-8-RIKEN, Mikazuki, Hyogo 679-5148, Japan*

(Received 30 March 2001; accepted for publication 6 August 2001)

An ultrahigh-resolution x-ray crystal monochromator providing a $120 \mu\text{eV}$ bandwidth at 14.41 keV is presented. The design, which uses four independent silicon crystals and has an output beam parallel to the incident beam, may be generalized to arbitrary energies. Fluxes of 1.3×10^6 photons/s (1.0×10^7 photons/s) in bandwidths of $120 \pm 15 \mu\text{eV}$ ($140 \pm 15 \mu\text{eV}$) were measured. The performance of the monochromator, including the preservation of coherence through it, was verified by measurement of a $9.6 \pm 2.0\%$ enhancement in the coincidence rate (i.e., $\gamma^{(2)} - 1 = 0.096 \pm 0.020$) in an intensity correlation experiment. © 2001 American Institute of Physics.
[DOI: 10.1063/1.1406925]

I. INTRODUCTION

In the x-ray region, production of a highly monochromatic beam is important for nuclear resonant scattering,¹ inelastic scattering,² and interferometry with good temporal coherence. In particular, the temporal coherence length ($\sim \lambda^2/\Delta\lambda$) at 10 keV is still an order of 1 mm even with a resolution $\Delta E/E (= \Delta\lambda/\lambda)$ of 10^{-7} . Further extension of coherence length may stimulate the development of x-ray interference techniques, while the available photon flux will inevitably be reduced by higher monochromatization. However, the recent development of brilliant x-ray sources, which are based on undulator radiation at the third-generation synchrotron facilities, such as ESRF, APS, and SPring-8, offers unprecedented opportunities for providing sufficient flux for practical applications even at an extremely monochromatic condition.

High-resolution crystal monochromators with resolution $(\Delta E/E) \sim 10^{-7} - 10^{-8}$ can be made in essentially two distinct ways. On one hand, a single reflection at a Bragg angle $\sim \pi/2$ can be used.³ On the other, multiple-bounce reflections, including asymmetric diffractions in most cases, may be employed.⁴⁻¹⁰ The $\sim \pi/2$ reflection design has the advantage of high efficiency with large angular acceptance, but limits one to specific energies determined by the lattice constant of the crystal employed, and to specific bandwidths, as determined by the intrinsic width of the reflection used.^{3,11} The multiple-bounce schemes offer more flexibility, including selection of nearly any energy (not only the energies of $\sim \pi/2$ reflections) and the capability to tailor the resolution at a specific energy. In particular, the best resolution previously

obtained at 14.41 keV [bandwidths of 0.92 (Ref. 9) and 0.65 meV (Ref. 10)] have used a $(+n, +n)$ two-bounce geometry with silicon asymmetric reflections (suitable $\sim \pi/2$ reflection is not available at this energy in silicon). However, this monochromator geometry has a resolution limit that follows from total external reflection when the asymmetric cuts of the crystals become large.^{9,12} This limit has been evaluated to be $\sim 300 \mu\text{eV}$ by Toellner *et al.*⁹ for 14.41 keV x rays and silicon crystals. In addition, the two-bounce geometry causes unwanted deflection of the exit beam direction. To avoid deflection, $(+n, +m, -m, -n)$ four-bounce geometry employing two channel-cut crystals has been utilized,^{5,6} where the exit beam is parallel to the incident beam (in-line geometry). Although this energy resolution is theoretically equivalent to that of $(+n, +m)$ two-bounce geometry, two channel-cut geometry may degrade the resolution, because of an imperfect surface finish originating from the complicated crystal design, and the possible mismatch of lattice constants between a pair of diffracting planes due to the thermal load of the incident radiation.¹³

In this article, we present a new ultrahigh-resolution monochromator (UHRM) with in-line geometry, which is applicable at arbitrary photon energy. The principle design details and test results are described and discussed. An application using monochromatic x rays with good temporal coherence is also presented.

II. PRINCIPLE

The basic idea (see Fig. 1). is to combine a couple of plane-wave optics:¹⁴ First a pair of asymmetric reflections $(+n, -n)$ generates a plane wave (~ 60 nrad divergence for the case here) and then a second pair of reflections $(-n,$

^{a)}Electronic mail: yabashi@sp8sun.spring8.or.jp

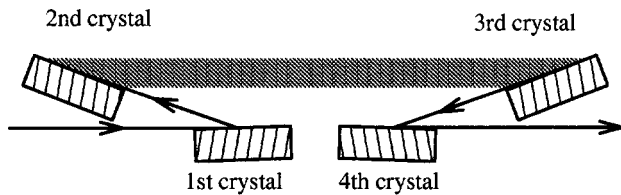


FIG. 1. Schematic of the UHRM.

$+n$) with opposite asymmetry selects a narrow bandwidth. This leads to an in-line geometry that also avoids the bandwidth limit mentioned above. We assume, for simplicity, that the asymmetry factors of the third and the fourth reflections, b_3 and b_4 , are equal to $1/b_2$ and $1/b_1$, respectively. According to a DuMond diagram analysis (Fig. 2),¹⁵ the energy resolution is approximately given by

$$\frac{\Delta E}{E} \approx P \sqrt{b_1 b_2} \omega_s \cot \theta_B \quad (1)$$

where θ_B , ω_s , and P are the Bragg angle, the Darwin width, and a polarization factor, respectively. The resolution of Eq. (1) is better than that of the $(+n, +n)$ geometry mentioned above by a factor of b_2 , which is what allows one to get much higher resolution.

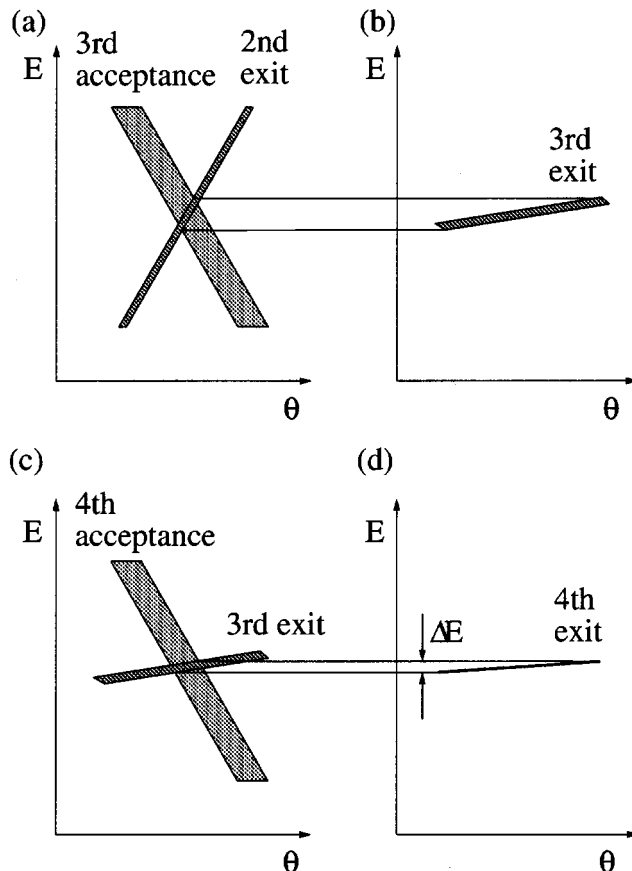


FIG. 2. Schematic DuMond diagrams for the incident beam for the third crystal (a), the exit from the third crystal (b), the incidence for the fourth crystal (c), and the exit from the fourth crystal (d).

III. DESIGN

We have built a monochromator to operate at 14.41 keV.¹⁶ It uses four Si 1153 reflections ($\theta_B = 80.4^\circ$, $\omega_s = 1.8 \mu\text{rad}$) with asymmetric angles of $\alpha = 78.4^\circ$. The corresponding asymmetric factor is $b = 1/10.4$ [i.e., $b = b_1 = b_2 = 1/b_3 = 1/b_4 = \sin(\theta_B - \alpha)/\sin(\theta_B + \alpha)$]. The theoretical resolutions, based on numerical calculations including proper absorption in crystals, are $\Delta E = 102 \mu\text{eV}$ for σ polarization ($P = 1$) and $97 \mu\text{eV}$ for π polarization ($P = 0.94$) in the full widths at half maximum (FWHM).

Details of the design of such a precision monochromator is crucial to its performance. One important point is our use of four independent flat crystals. This facilitates a good surface finish which is indispensable for high-resolution and preservation of the coherence, especially when highly asymmetric reflections are employed. It also allows us to compensate for angular deviation due to refraction from the asymmetric reflections¹⁷ ($\sim 75 \mu\text{rad}$ in our case), and for temperature shifts between crystals, by independent angular adjustments. The four crystals were cut to $30 \times 25 \times 10 \text{ mm}^3$ ($L \times W \times T$, where the dimensions are L in the scattering plane, W perpendicular to the plane, and thickness T) from a floating zone (FZ) silicon ingot. This allows an UHRM spatial acceptance of $0.1 \times 25 \text{ mm}^2$ [$Lb \tan(\theta_B - \alpha) \times W$]. During cutting, the crystal orientations were adjusted to within 0.05° using a diffractometer. The crystals were chemically etched to remove damage from the cutting and then mechanochemically polished for a fine surface finish.

IV. RESULTS AND DISCUSSION

The UHRM was tested at SPring-8 using a 25 m long undulator beamline, 19LXU.¹⁸ The 14.41 keV first harmonic of the undulator radiation was premonochromatized with a cryogenically cooled double-crystal silicon (111) monochromator. The UHRM was installed in a separate hut, located at $\sim 67 \text{ m}$ from the center of the undulator. The hut room temperature was stabilized to 0.1 K with a precise temperature controller and a vinyl cover was placed over an experimental table for further temperature stabilization and to avoid air flow. The UHRM crystals were controlled with two coaxial precision goniometers⁵ (12.2 nrad step size), for a total of four independent, high-resolution axes. A horizontal scattering plane was used (π polarization) for convenience in the subsequent intensity correlation experiment. The crystals were placed on aluminum crystal mounts, without glue, to avoid possible crystal strain. Small stages were attached between the crystal mounts and the rotation stages in order to control the tilt of the crystals. These enabled the diffracting lattice vectors to be aligned to within $120 \mu\text{rad}$ of horizontal by measuring the vertical deviation of the diffracted beam.

We used nuclear forward scattering¹⁹ (NFS) to measure the energy resolution. The fourth crystal was rotated while detecting the NFS delayed signals of ^{57}Fe with an avalanche photodiode (APD). According to a DuMond analysis, the energy shift is given by

$$\frac{\Delta E}{E} = \frac{1}{2b_3} \Delta \theta_4 \cot \theta_B, \quad (2)$$

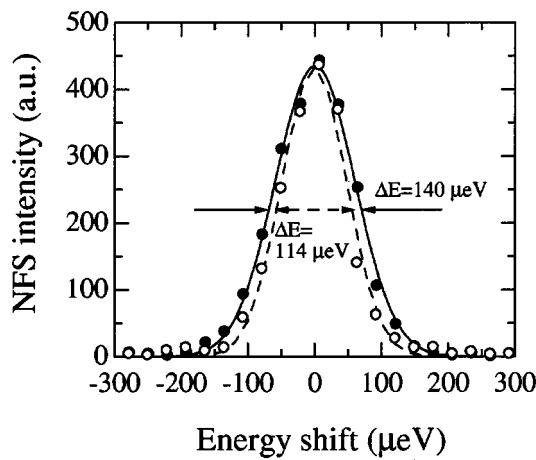


FIG. 3. Measured NFS profiles, as a function of the energy shift by fourth crystal rotation, with a slit size of 500×92.5 (closed circles) and 100×22.5 μm^2 (open circles). The solid and dashed lines show the fits with Gaussian distributions, and the arrows indicate the full widths at half maximum.

as a function of the fourth crystal rotation angle, $\Delta\theta_4$.²⁰ Figure 3 shows typical NFS intensity profiles with an entrance slit size of 500×92.5 μm^2 (vertical \times horizontal, closed circles) and 100×22.5 μm^2 (open circles). With repetitive rotations in opposite directions, the bandwidths ΔE were determined to be 140 ± 15 and 120 ± 15 μeV for each slit size. The latter corresponds to an energy resolution $\Delta E/E$ of 8×10^{-9} . The uncertainty of the bandwidths (as determined from the variation in successive measurements) may originate from a slow energy drift due to a temperature or angular shift of the UHRM crystals. The narrower bandwidth measured is ~ 1.2 times larger than the theoretical value, 97 μeV . We also observed that the bandwidth gets broader for larger slits. It seems that the broadening is caused mainly by crystal lattice imperfections within a diffraction volume. If we assume that both the broadening profile and the intrinsic energy profile are represented as Gaussian distributions, the bandwidth broadening due to imperfections is estimated to be 71 μeV for $\Delta E = 120$ μeV . This corresponds to a lattice spacing variation of $\Delta d/d = 5 \times 10^{-9}$.

The photon flux that emerged from the UHRM was found to be 1.0×10^7 photons/s at 98.8 mA (140 μeV bandwidth, 500×95 μm^2 slit) while the incident flux (2.1 eV bandwidth) was 3.4×10^{12} photons/s for the same slit size.²¹ This corresponds to spectral efficiency in the unit area (ratio of photons/s/bandwidth/ mm^2) of 4.4%, which is 65% of the calculated value, 6.8%.²² The efficiency obtained is reasonable when the bandwidth broadening from the theoretical value (140/97 μeV) is taken into account. For the smaller slit size (100×22.5 μm^2), photon flux of 1.3×10^6 photons/s was measured.

The UHRM efficiency is inevitably low because four higher-order reflections are used. The maximum reflectivity R for the single reflections is calculated to be 0.67 with a Debye–Waller factor of 0.56. The four bounces reduce the peak reflectivity to $R^4 = 0.20$. Furthermore, the angular acceptance which is calculated as 6.4 μrad (and may be estimated approximately as $b_1^{-1/2} P \omega_s$) is smaller than the angular divergence of the incident beam. To solve these problems,

a $(+m, -m, -n, +n)$ arrangement may be considered. By making the $(+m, -m)$ reflections of low order, one may improve the acceptance and efficiency at the expense of slight degradation in the energy resolution. We note that, even with the present design, one can increase the total photon flux using a vertical scattering plane²¹ or one combined with a refractive collimator.^{10,23}

V. APPLICATION

In order to investigate the coherence of the monochromatic beam, we performed an x-ray intensity correlation experiment,^{24,25} similar to the work of Hanbury-Brown and Twiss.²⁶ A horizontal scattering plane was used to allow us to match the UHRM acceptance to the spatial (transverse) coherence area of the incident beam (these are estimated to be ≥ 100 μm in the vertical and ≤ 10 μm in the horizontal). Additional equipment for these experiments included a silicon crystal in Laue geometry used as a beam splitter, two APDs, and a coincidence unit²⁷ with a delay circuit similar to that in Ref. 25. Here the degree of the second-order coherence, $\gamma^{(2)}$, can be obtained as the ratio C_S/C_N , where C_S denotes the coincidence rate for a single bunch and C_N the accidental rate (measured with an interval of a revolution time of the storage ring, 4.79 μs). We observed that $\gamma^{(2)}$ increased at smaller slit widths, as is expected from the chaotic photon statistics.²⁸ In particular, we preliminarily found $\gamma^{(2)} = 1.096$ for a slit size of 300×10 μm^2 . The high value indicates that the photons that emerged from the UHRM are highly coherent both in space and time. The statistical error $(C_S^{-1} + C_N^{-1})^{1/2}$ was 0.020 over a 1.5 h accumulation period. We note that the validity of the circuit was confirmed by the coincidence measurements without using the UHRM, where $\gamma^{(2)}$ was 1.0003 ± 0.003 . More details of the intensity correlation experiment will be reported elsewhere.

ACKNOWLEDGMENT

The authors are grateful to Dr. A. Q. R. Baron for valuable discussions and for the loan of ^{57}Fe foils.

¹ *Nuclear Resonant Scattering of Synchrotron Radiation*, edited by E. Gerdau and H. de Waard (Baltzer Science, Bussum, The Netherlands, 1999/2000).

² See, for example, E. Burkel, *Inelastic Scattering of X-rays with Very High Energy Resolution* (Springer, Berlin, 1991); F. Sette, M. H. Kirsch, C. Masciovecchio, G. Ruocco, and G. Monaco, *Science* **280**, 1550 (1998), and references therein.

³ W. Graeff and G. Materlik, *Nucl. Instrum. Methods Phys. Res.* **195**, 97 (1982); B. Dörner, E. Burkel, and J. Peisl, *Nucl. Instrum. Methods Phys. Res. A* **426**, 450 (1986); R. Verbeni *et al.*, *J. Synchrotron Radiat.* **3**, 62 (1996).

⁴ G. Faigel, D. P. Siddons, J. B. Hastings, P. E. Hausteijn, J. R. Grover, J. P. Remeika, and A. S. Cooper, *Phys. Rev. Lett.* **58**, 2699 (1987).

⁵ T. Ishikawa, Y. Yoda, K. Izumi, C. K. Suzuki, X. W. Zhang, M. Ando, and S. Kikuta, *Rev. Sci. Instrum.* **63**, 1015 (1992).

⁶ T. S. Toellner, T. S. Mooney, S. Shastri, and E. E. Alp, *Proc. SPIE* **1740**, 218 (1992).

⁷ D. P. Siddons, U. Bergmann, and J. B. Hastings, *Phys. Rev. Lett.* **70**, 359 (1993).

⁸ A. I. Chumakov, J. Metge, A. Q. R. Baron, H. Grünsteudel, H. F. Grünsteudel, R. Rüffer, and T. Ishikawa, *Nucl. Instrum. Methods Phys. Res. A* **383**, 642 (1996).

- ⁹T. S. Toellner, M. Y. Hu, W. Sturhahn, K. Quast, and E. E. Alp, *Appl. Phys. Lett.* **71**, 2112 (1997).
- ¹⁰A. I. Chumakov, R. Rüffer, O. Leupold, A. Barla, H. Thiess, T. Asthalter, B. P. Doyle, A. Snigirev, and A. Q. R. Baron, *Appl. Phys. Lett.* **77**, 31 (2000).
- ¹¹K. Kohra and T. Matsushita, *Z. Naturforsch. Teil A* **27A**, 484 (1972).
- ¹²S. Kimura, J. Harada, and T. Ishikawa, *Acta Crystallogr., Sect. A: Found. Crystallogr.* **50**, 337 (1994).
- ¹³We note that A. Q. R. Baron *et al.* recently developed a compact in-line HRM with four-bounce reflections including Bragg angles $\sim \pi/2$, where these problems are sophisticatedly solved. [A. Q. R. Baron, Y. Tanaka, D. Ishikawa, D. Miwa, M. Yabashi, A. I. Chumakov, and T. Ishikawa, *J. Synchrotron Radiat.* **8**, 1127 (2001)].
- ¹⁴K. Kohra and K. Kikuta, *Acta Crystallogr., Sect. A: Cryst. Phys., Diffraction, Gen. Crystallogr.* **24**, 200 (1968); T. Ishikawa, *Acta Crystallogr., Sect. A: Found. Crystallogr.* **44**, 496 (1988).
- ¹⁵J. W. M. DuMond, *Phys. Rev.* **52**, 872 (1937); K. Nakayama, H. Hashizume, A. Miyoshi, S. Kikuta, and K. Kohra, *Z. Naturforsch. Teil A* **28**, 632 (1973).
- ¹⁶This energy was chosen for convenience in measuring the bandwidth via scattering from the nuclear resonance in ^{57}Fe .
- ¹⁷S. Kikuta and K. Kohra, *J. Phys. Soc. Jpn.* **29**, 1322 (1970).
- ¹⁸M. Yabashi *et al.*, *Nucl. Instrum. Methods Phys. Res. A* **467–468**, 678 (2001).
- ¹⁹J. B. Hastings, D. P. Siddons, U. van Bürcck, R. Hollatz, and U. Bergmann, *Phys. Rev. Lett.* **66**, 770 (1991).
- ²⁰In general, the resolution measurement using NFS with crystal rotation is valid when the energy spectrum of the incident beam for the rotated crystal (fourth crystal in our case) is sufficiently larger than the spectrum of the exit beam from the crystal. For our case, this condition was verified not only by the DuMond diagram analysis theoretically (Fig. 2), but also by the rocking curve measurements experimentally, where the rocking curve width for nonresonant signal ($\sim 6 \mu\text{rad}$) was sufficiently larger than that for NFS signal ($\sim 1 \mu\text{rad}$).
- ²¹Incident flux without the slit is estimated to be 6×10^{13} photon/s with a beam size of $0.5(\text{V}) \times 1.3(\text{H}) \text{ mm}^2$ (FWHM) at the monochromator position. Apart from the decrease of the throughput discussed in the text, the throughput was reduced by a factor of ~ 15 because of the spatial acceptance of the HRM limited in the horizontal direction.
- ²²For the calculation, a horizontal angular source size of $13.0 \mu\text{rad}$ (FWHM) seen from the UHRM position is used as an incident angular divergence, because the UHRM spatial acceptance is sufficiently smaller than the horizontal source size, 0.87 mm (FWHM).
- ²³A. Q. R. Baron, Y. Kohmura, Y. Ohishi, and T. Ishikawa, *Appl. Phys. Lett.* **74**, 1492 (1999); *J. Synchrotron Radiat.* **6**, 935 (1999).
- ²⁴E. Ikonen, *Phys. Rev. Lett.* **68**, 2759 (1992).
- ²⁵Y. Kunimune, Y. Yoda, K. Izumi, M. Yabashi, X. W. Zhang, T. Harami, M. Ando, and S. Kikuta, *J. Synchrotron Radiat.* **4**, 199 (1997); E. Gluskin, E. E. Alp, I. McNulty, W. Sturhahn, and J. Sutter, *ibid.* **6**, 1065 (1999).
- ²⁶R. Hanbury-Brown and R. Q. Twiss, *Nature (London)* **177**, 27 (1956).
- ²⁷During the experiment the SPring-8 storage ring was operated in 406 bunch mode with a bunch interval of 11.8 ns, which is sufficiently larger than the time resolution of the coincidence unit (Phillips Scientific Research, 754) used here. Actually, 32 buckets of 406 buckets were operated as empty bunches in order to avoid instability of orbital electrons, although this did not affect our experiment.
- ²⁸L. Mandel and E. Wolf, *Optical Coherence and Quantum Optics* (Cambridge University Press, Cambridge, 1995).